This is an open access article published under an ACS AuthorChoice License, which permits copying and redistribution of the article or any adaptations for non-commercial purposes.

Environmental Science & Technology

Article

pubs.acs.org/est

Speciation and Reactivity of Uranium Products Formed during *in Situ* Bioremediation in a Shallow Alluvial Aquifer

Daniel S. Alessi,[†,⊗] Juan S. Lezama-Pacheco,[‡] Noémie Janot,[‡] Elena I. Suvorova,[†] José M. Cerrato,[§,#] Daniel E. Giammar,[§] James A. Davis,[∥] Patricia M. Fox,[∥] Kenneth H. Williams,[∥] Philip E. Long,[∥] Kim M. Handley,[⊥,∇] Rizlan Bernier-Latmani,[†] and John R. Bargar*[,‡]

[†]Environmental Microbiology Laboratory, Ecole Polytechnique Fédérale de Lausanne, CH-1015, Lausanne, Switzerland

[‡]Chemistry and Catalysis Division, Stanford Synchrotron Radiation Lightsource, SLAC National Accelerator Laboratory, Menlo Park, California 94025, United States

[§]Department of Energy, Environmental, and Chemical Engineering, One Brookings Drive, Washington University, Saint Louis, Missouri 63130, United States

[∥]Earth Sciences Division, Lawrence Berkeley National Laboratory, 1 Cyclotron Road, Berkeley, California 94720, United States

[⊥]Department of Earth & Planetary Sciences, University of California, Berkeley, California 97420, United States

Supporting Information

ABSTRACT: In this study, we report the results of *in situ* U(VI) bioreduction experiments at the Integrated Field Research Challenge site in Rifle, Colorado, USA. Columns filled with sediments were deployed into a groundwater well at the site and, after a period of conditioning with groundwater, were amended with a mixture of groundwater, soluble U(VI), and acetate to stimulate the growth of indigenous microorganisms. Individual reactors were collected as various redox regimes in the column sediments were achieved: (i) during iron reduction, (ii) just after the onset of sulfate reduction, and (iii) later into sulfate reduction. The speciation of U retained in the sediments was studied using X-ray absorption spectroscopy, electron microscopy, and chemical extractions. Circa 90% of the total uranium was reduced to U(IV) in each reactor. Noncrystalline U(IV) comprised about two-thirds of the U(IV) pool, across large changes in microbial community structure, redox regime, total uranium accumulation, and reaction time. A significant body of recent research has demonstrated that noncrystalline U(IV) species are more suceptible to remobilization and reoxidation than crystalline U(IV) phases such as uraninite. Our results highlight the importance of considering noncrystalline U(IV) formation across a wide range of aquifer parameters when designing *in situ* remediation plans.

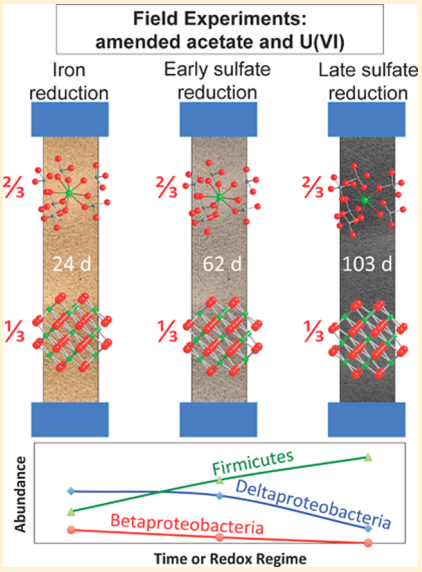

1. INTRODUCTION

Microbiological strategies for the immobilization of dissolved uranium in aquifers focus on the addition of exogenous electron donors to stimulate growth of the indigenous microbial community.[1] U(IV) products observed in laboratory and field U(VI) reduction experiments include biogenic uraninite [UO_{2+x}(s)] nanoparticles[2,3] and a variety of noncrystalline U(IV) products, including U(IV) coordination polymers associated with biomass[4−8] and U(IV) monomers associated with Fe(II)-bearing minerals and titanium dioxide.[9−11] The discovery of non-uraninite forms of U(IV) in bioreduced field sediments[7] is a key development in the field of uranium bioremediation because these species are less stable than uraninite in the presence of dissolved carbonate species and oxygen.[12]

Although the products of uranium reduction are increasingly well documented in the laboratory, their dependence upon specific types of geochemical conditions and microbial metabolisms prevalent in the field has received comparatively less attention.[13] Bargar et al.[7] examined the products of U(VI) reduction in whole sediments bioreduced in the aquifer at the U.S. Department of Energy field research site at Rifle, Colorado, after 90 days of biostimulation, at which point "deep" sulfate-reducing conditions had been achieved (i.e., conditions characterized by reduction of ca. 8−10 mM sulfate to sulfide). Acetate stimulation of the Rifle aquifer leads to the

Received: June 3, 2014
Revised: September 16, 2014
Accepted: September 29, 2014
Published: September 29, 2014

 © 2014 American Chemical Society

Table 1. Experimental Parameters for *in Situ* Columns

manuscript column name	T1	–	–	T2	T3
field column name	2B	2D	2E	4A	4E
duration: preconditioning groundwater elution (d)	19	19	19	19	19
field acetate amendment start[a] (day number)	0	0	0	0	0
uranyl column amendment (20 μM) start (day number)	1	1	1	47	47
acetate column amendments concentration (mM)	3	3	3	13[b] (at 47 d)	13[b] (at 47 d)
dominant biogeochemical regime	iron reduction	iron reduction	iron reduction	sulfate reduction	sulfate reduction
duration of acetate column amendment (d)	24	24	24	61	102
duration of uranyl column amendment (d)	24	24	24	15	56

[a]August 23, 2010. [b]Columns received up to 3 mM acetate from groundwater during the field acetate amendment.

onset of predominantly metal-reducing conditions, followed by development of sulfate-reducing conditions after a lag time of ca. 10−40 days,[14] with shorter periods observed if the well gallery had previously been biostimulated. Microbial community structure and groundwater/sediment geochemistry under these conditions contrast strongly. For example, in metal-reducing conditions, aqueous Fe(II) species accumulate to concentrations exceeding 100 μM, and planktonic metal-reducing bacteria are abundant, whereas in sulfate-reducing conditions Fe(II) is sequestered in solid iron sulfide precipitates while sulfate-reducing bacteria and aqueous sulfide species begin to dominate.[14] In particular, abiotic reduction often produces uraninite, whereas biological U(VI) reduction in axenic culture often produces a mixture of noncrystalline U(IV) and uraninite. These differences led us to hypothesize that U(IV) products may vary in structure and stability in response to microbial community structure and redox chemistry. Ultimately the reactivity of U(IV) in the field is controlled by its speciation. Thus, characterizing U(IV) products formed as aquifer biogeochemical conditions progress is critical to designing effective field remediation schemes and provides insights to understand naturally occurring U(VI) bioreduction.

The objective of this study was to determine the effect of the predominant biogeochemical redox regime on the products of U(VI) bioreduction under field-relevant conditions. To do so, we deployed reactors filled with fresh sediments from Rifle, CO, into groundwater wells at the field research site during the 2010 "Super 8" acetate biostimulation field experiment. The reactors were continuously eluted with the surrounding groundwater prior to and throughout the field experiment to biogeochemically couple them to the surrounding aquifer. Reactors were sacrificed during late iron reduction and early and mid sulfate reduction, allowing us to compare the U(IV) products and their reactivity under contrasting biogeochemical conditions. Extended X-ray absorption fine structure (EXAFS), chemical extraction,[15] and electron microscopy were used to characterize the uranium products formed.

2. METHODS

2.1. 2010 *in Situ* Field Experiments. Sediments were collected at the Integrated Field Research Challenge (IFRC, Rifle, Colorado, USA) field site from below the water table with a backhoe on July 28, 2010, sieved in the field to <2 mm, and homogenized in the process. The sediments were denoted as the "Super 8 composite".[16] Sediments were stored moist in nitrogen-purged aluminized mylar bags at 4 °C before being packed into borosilicate glass chromatography columns (Kontes) measuring 2.6 cm in diameter and 15 cm in length (approximately 80 cm^3 of sediments). Acid digestion of the Super 8 composite (*vide infra*) showed that it contains only trace concentrations of U ($(8.0 \pm 2.4) \times 10^{-3}$ μmol U g^{-1} sediment; see Figure 3). The in-well column field experiments were conducted using a design similar to those reported by Moon et al.[17] and Bargar et al.[7] Specifically, reactors were deployed into groundwater well CD-04 in the experimental plot C well gallery on August 4, 2010 (Supporting Information, Figure SI-1), located approximately 100 m from the Super 8 composite collection site. The water table depth at the Rifle site varies between approximately 9 and 12 ft below ground surface (BGS), and the columns were placed at 14−17 ft BGS to guarantee they remained submerged throughout the experiment. The Rifle aquifer has low but measurable amounts of dissolved oxygen (DO),[18] typically <0.2 ppm.[19] Once deployed below the water table and prior to acetate amendment, CD-04 groundwater from a depth of approximately 17 ft BGS was pumped through the reactors at a nominal rate of 16.8 mL h^{-1}, representing a Darcy velocity of 9.5×10^{-6} m s^{-1}, for 19 d to recondition the sediments to the aquifer chemistry and microbiology. Subsequently, on August 23, 2010, amendment of the entire experimental plot C well gallery with 3 mM acetate commenced[20,21] (Table 1; Supporting Information, Figure SI-2). Added acetate and uranium (<1 μM) present within the aquifer reached the columns via groundwater eluted through the columns. To ensure that sediment uranium concentrations would be adequate for spectroscopic and microscopic analysis, the reactors received supplemental acetate (3 mM) and uranyl (20 μM) amendments beginning on August 24, 2010. This uranium concentration falls within the range of historical groundwater U(VI) values at contaminated sites in the Colorado River basin (<ca. 50 μM).[22] Amendments were made by mixing acetate and a 200 μM stock solution of uranyl acetate in groundwater at a 1:10 dilution to the influent groundwater.

The columns were harvested from the well at three times, designated as T1−T3 (Table 1), corresponding to increasing time in the well, increasing acetate amendment duration, and therefore more reducing conditions. Prior acetate biostimulation experiments at the Rifle IFRC site provided valuable information about when redox transitions would occur in the aquifer (e.g., refs 7, 17, 23, 24), which was used to pre-plan harvest dates. T1 reactors received acetate and uranium amendments for 24 d, after which uranyl additions were halted, and they were eluted with groundwater for 7 d at 60 mL h^{-1} to flush out unreduced U(VI) species. All T1 reactors were harvested at the peak of Fe(II) concentrations (i.e., under late iron-reducing conditions) (8 mg L^{-1}, Figure SI-2) and shipped to Stanford Synchrotron Radiation Lightsource (SSRL) under anoxic conditions for further analysis. Reactors T2 and T3, targeted for sulfate-reducing conditions, were initially amended with the field experiment acetate plume to advance them

through the iron-reducing phase and into early sulfate reduction. Subsequently, they were amended with 13 mM acetate and 20 μM uranyl acetate, starting on October 9, 2010, 47 d after acetate amendment began in the experimental plot C gallery and when HS^- was present in well CD-04. By waiting to amend with uranyl until sulfate-reducing conditions had already begun, we were able to avoid significant "contamination" of the column sediments by U(IV) produced under preceding iron-reducing conditions. We are thus able to make a "head-to-head" comparison of "iron-reduced" and "sulfate-reduced" U(IV) products. By using 13 mM acetate, we were able to ensure that sulfate-reducing bacteria (SRB) did not consume all of the added acetate, and therefore *Geobacter* could be available to reduce U(VI) throughout. This design was chosen as a foundation for a future experiment (not yet performed) in which lower acetate conditions will be completely consumed by SRB. The reactor T2 amendment lasted 15 d, after which uranyl amendments were halted, and T2 was eluted with groundwater as described above and recovered. The reactor T3 amendment extended for a total of 56 d, and subsequently T3 was flushed with groundwater for 6 d prior to recovery.

During recovery from the aquifer, pre-installed valves located directly above and below the columns were closed to isolate the colums from inlet/outlet lines for removal. Within 5−10 min, the entire intact columns were placed in hermetically sealed stainless steel shipping containers, which were purged with N_2 gas. The glass column walls, end-caps, and rapid handling procedures prevented oxygen intrusion. Columns were shipped overnight to SSRL in the purged stainless-steel containers. Column sediments were divided into top (effluent) and bottom (influent) sections, transferred into stoppered serum bottles under 5% H_2/95% N_2 atmosphere at SSRL, and frozen at −40 °C to halt any further biogeochemical reactions.

2.2. Groundwater Characterization. Groundwater samples were collected from well CD-04 and other wells in the experimental plot C gallery several times per week during the experimental period (August to November, 2010) and analyzed to determine the concentrations of a broad suite of anions and cations, dissolved acetate (Figure SI-2), electrical conductivity, DO, and pH. Details of these analytical methods can be found in the work of Williams et al.[20]

2.3. Chemical Extractions. Total uranium in the sediments was determined by digestion using aqua regia, comprised of a 1:3 mixture of 15 M HNO_3 and 12 M HCl. Prior to digestion, sediments were dried in a N_2(g) environment for 24 h at ambient temperatures to normalize water content. Approximately 1 g of dried sediment (weighed precisely in each case) was placed into 5 mL of oxic aqua regia and allowed to react for 48 h. Duplicate digestions were performed for each condition. Aliquots of the digest were filtered through 0.22 μm membranes and diluted as needed in 0.1 N HNO_3, and total U was measured using inductively coupled plasma mass spectrometry (ICP-MS; Perkin-Elmer ELAN DRC II).

The noncrystalline U(IV) fraction of the total reduced U pool in the sediments was determined by extraction with 1 M sodium bicarbonate solutions.[15] In an anaerobic chamber containing 97% N_2/3% H_2, a precisely weighed sample of each sediment (approximately 1 g in all cases) was reacted with 10 mL of anoxic 1 M bicarbonate for 24 h. Bicarbonate extractions were performed in triplicate. An aliquot of each supernatant was filtered through a 0.22 μm membrane, and 0.5 mL of supernatant was dissolved into 4.5 mL of oxic 1 M HNO_3 to rapidly oxidize noncrystalline U(IV) extracted into the bicarbonate solution. The resulting solution was further diluted into 0.1 M HNO_3 as necessary for ICP-MS measurements of total U. The noncrystalline U(IV) fraction of the total U pool was taken to be the U measured in the bicarbonate extractions. Remaining U, calculated by subtracting the noncrystalline U(IV) fraction from the total U determined by aqua regia digestion, was interpreted as crystalline U(IV) or UO_2(s). An aqua regia digest of the initial column sediment, prior to acetate and uranyl amendment, showed that it contains a negligible amount of uranium (see Figure 3).

Stoliker et al.[25] showed that in some cases U(IV) species extracted from sediments using a 1 M anoxic bicarbonate solution may be rapidly oxidized, even in the absence of oxygen. To test for the possibility of U(IV) oxidation following bicarbonate extraction, the potential presence of adsorbed U(VI) on the sediments, or a solid U(VI) phase associated with reactor sediments, a separate 20 μL aliquot of the filtered anoxic supernatants (see above) was mixed with 1.98 mL of anoxic 1 M HNO_3 and immediately analyzed using a kinetic phosphoresence analyzer. In these control experiments, no uranyl was detected as extracted from the sediments. This result correlates well with X-ray absorption near-edge structure (XANES) measurements of the same sediments (Supporting Information, Figure SI-4), which are commonly accepted to have an error of approximately 10%.[26]

2.4. Microbial Community Analyses. *2.4.1. DNA Extraction, Amplification, and Sequencing.* Genomic DNA was extracted from 5 g of sediment per sample and amplified using universal bacterial 16S rRNA gene primers 27F and 1492R, following methods described by Handley et al.[27] After amplification, *Leptospirillum ferrodiazotrophum*[28] 16S rRNA gene amplicons were spiked into samples at 0.5% final concentration to serve as a control. Amplicons were fragmented to an average size of 300 bp, and Illumina libraries were prepared as described by Handley et al.[27] Barcoded libraries were pooled and sequenced on one-sixth of an Illumina HiSeq2000 flow cell (Illumina, Inc., San Diego, CA, USA), and 100 bp long paired-end reads were collected.

Reads were trimmed to remove low-quality bases and assembled into (nearly) full-length 16S rRNA gene sequences using the EMIRGE (Expectation Maximization Iterative Reconstruction of Genes from the Environment) method for 16S rRNA gene amplicons.[29] Briefly, 1 million randomly sampled reads per sample were reconstructed into full-length 16S rRNA genes over 100 EMIRGE iterations, and after initial read mapping to a de-replicated version of the SILVA 108 16S rRNA database (http://www.arb-silva.de/). During reconstruction, sequences were clustered into operational taxonomic units (OTUs) based on similarities of ≥97%. OTU abundances, calculated on the basis of the number of mapped reads, were normalized to account for varying sequence lengths. To exclude unreliable rare sequences, only OTUs with raw relative abundances ≥0.01% were used in analyses. This resulted in 334−909 OTUs per sample.

2.4.2. Phylogenetic Analyses. Representative OTU sequences were analyzed using the Ribosomal Database Project (RDP, release 10) naïve Baysian classifier,[30] in order to assign taxonomy. For comparison, OTUs were BLASTed[31] against the SILVA 16S rRNA database in order to determine sequence identities. Sequences from all samples were aligned together using SSU-ALIGN 0.1 (http://selab.janelia.org/software/ssu-align) and masked to remove inserted columns (which do not contain aligned nucleotides) as well as regions of low alignment

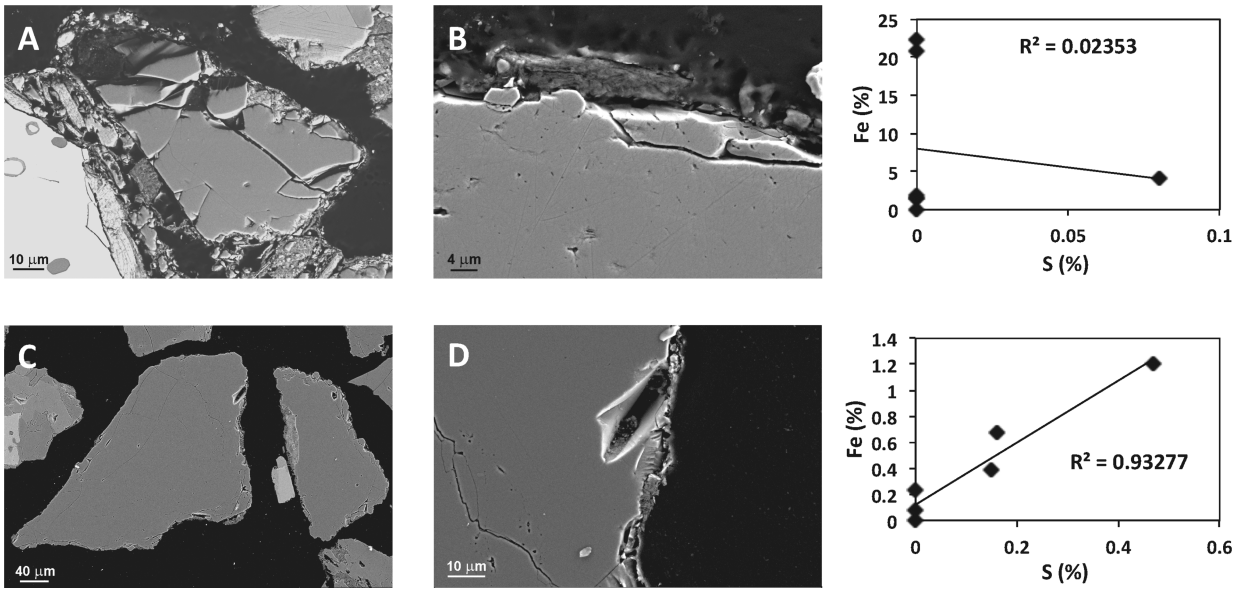

Figure 1. SEM images with selected area energy-dispersive X-ray spectroscopy (EDS) data, evidencing the development of FeS coatings on silica mineral grains in biostimulated sediments: (A,B) preamendment or Super 8 composite sediment and (C,D) sulfate-reducing conditions in column T3 sediments (influent end of column). A well-developed Fe:S ratio is observed in sulfate-reducing conditions (inset plots of EDS data).

confidence, which were determined by the calculation of posterior probabilities based on alignment to a covariance model. An approximately maximum-likelihood phylogenetic tree was generated using FastTree 2.0.1.[32] The tree was rooted to *Thermus thermophilus* (X07998.1). Sample communities were compared using phylogenetic (tree-based) and OTU abundance information with weighted Fast UniFrac.[33] Data were analyzed with and without normalization, which accounts for potential differences in OTU branch length owing to different rates of organism evolution.

2.4.3. Accession Numbers. 16S rRNA gene sequences were deposited in GenBank under the accession numbers JX221725−JX226064.

2.5. Electron Microscopy. Unreacted Super 8 composite sediment and sediment samples from reactors T1−T3 were fixed in epoxy (EpoTek 301) in an anaerobic chamber, from which 30 μm thick petrographic thin sections mounted on glass were made (Spectrum Petrographics, Vancouver, WA). Scanning electron microscopy (SEM) and X-ray energy-dispersive spectrometry (EDS) were performed on a Carl Zeiss MERLIN (Oberkochen, Germany) microscope at 3−10 kV accelerating voltages in secondary electron imaging mode for sediment grains imaging and their chemical analysis. Quantification of elements was done using an INCA X-ray EDS system (Oxford). SEM images were collected from more than 80 individual grains, and from those, EDS measurements of elemental composition were made on more than 350 individual points. For column T3, which entered into sulfate-reducing conditions, 137 measurements were made at grain boundaries, and Fe and S were co-present at 107, or 77.4% of these points.

2.6. X-ray Absorption Spectroscopy (XAS). U L-edge EXAFS spectra were measured at beamline 11-2 of the SSRL at the Stanford Linear Accelerator Laboratory (SLAC) to characterize the average molecular structure around uranium in bulk sediments. Sediments were mounted into aluminum holders covered with Kapton windows in an anaerobic chamber and mounted in a cryostat cooled with liquid nitrogen to 77 K to improve data quality. A double-crystal Si (220) monochromator was used for energy selection, detuned 15−30% to reject higher harmonic intensities. Y and Mo foils were used to continuously monitor beamline energy calibration. Beamline energy resolution was controlled at much less than the U L_{III}- or L_{II}-edge line width (8.67 eV) using vertical slits. EXAFS oscillations were subtracted by fitting a smoothly varying function (spline) to remove contributions below 1.4 Å, which may result in non-physical pair correlations, using the SixPACK[34] and Horae[35] analysis packages. FEFF8.4 was used to calculate backscattering phase and amplitude functions used to fit the spectra.[36] Further details of the EXAFS fitting procedures are given in the Supporting Information.

3. RESULTS AND DISCUSSION

3.1. Metal- and Sulfate-Reducing Conditions within Whole Sediment Reactors. Changes in the Fe and S mineralogy and the microbial communities in reactors T1−T3 demonstrate the shift to more reducing conditions. SEM images of silicate grains accompanied by EDS data (Figure 1) show that unstimulated Super 8 composite sediment has low concentrations of S (Figure 1A,B) around the grain surfaces, and no correlation is observed between these elements. In contrast, grains from reactor T3 exhibit well-developed sulfidic coatings in which Fe:S are well correlated at a ratio just below unity (Figure 1C,D). The ratio of Fe:S in grain coatings in T3 less than 1:1 may be explained by the accumulation of elemental sulfur resulting from the oxidation of sulfide by U(VI) or the reaction between aqueous hydrogen sulfide species and iron oxides.[37,38] Additionally, a significant change in sulfide concentrations in the effluent of reactor T3, increasing from 0.014 mg L^{-1}, 30 days following field acetate amendment, to 0.733 mg L^{-1} after 70 days of field acetate amendment, was observed (Supporting Information, Table SI-2). Williams et al.[20] reported that elemental sulfur may form in Rifle sediments via abiotic oxidation of aqueous sulfide coupled to the reduction of goethite or other Fe(III)-bearing refractory minerals in the sediments. Furthermore, the development of

similar grain coatings was observed in biostimulated sediments at the Rifle site by Bargar et al.[7] after a much longer biostimulation period (90 d).

Microbial community analyses (Figure 2) record the transition in redox conditions observed in SEM imaging of sediment grains. Clear differences among communities correlate with the duration of acetate amendment and/or whether collected from the top (effluent) or bottom (influent) of columns (Figure 2). Communities collected from T1 reactors grouped together and separated from communities in reactors T2 and T3 (Figure 2; Supporting Information, Figure SI-3A,B). In contrast, communities collected at the Infl and Effl ends of reactor T2 were distinct from one another. The T2 Infl community was evidently more similar to the later T3 communities, in particular the T3 Effl community. The Rifle IFRC site is far from thermodynamic equilibrium; thus, nonequilibrium, kinetics-based approaches must be invoked to explain U transport at the site.[39] The column reactor sediments are also far from equilibrium conditions, which allows for redox heterogeneity along the length of the column (15 cm) and at the micrometer pore scale during acetate amendment.[7]

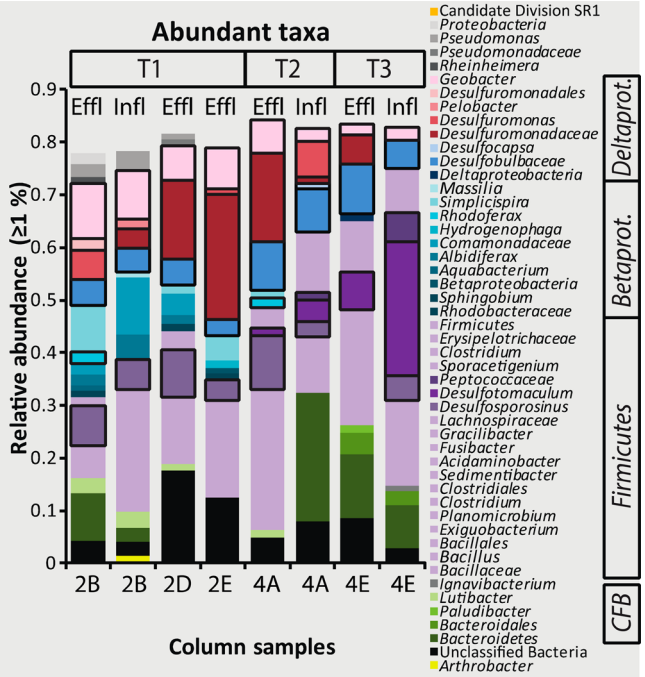

Figure 2. Microbial community analyses showing community composition of the most abundant taxa (>1% relative abundance) at the genus (or nearest taxonomic) level. "Effl" and "Infl" denote the top (effluent) and bottom (influent) ends the columns, respectively. Labels at the bottom correspond to individual field columns. Columns 2D and 2E are replicates of the 2B column. Black boxes demark potential Fe(III)- and sulfate-reducing taxa (i.e., *Geobacter* and other *Desulfuromonadales*; *Rhodoferax*; *Peptococcaceae* such as *Desulfosporosinus* and *Desulfotomaculum*; and *Desulfocapsa* and *Desulfobulbaceae*). Abbreviations: CFB, cytophaga flavobacterium bacteroidetes; Betaprot, Betaproteobacteria; Deltaprot, Deltaproteobacteria.

In terms of composition, there was an overall decrease in *Proteobacteria* and increase in *Firmicutes* with time (Figure SI-3C). Specifically, bacteria most closely related to *Geobacter*, other *Desulfuromonadales*, and *Rhodoferax* (*Betaproteobacteria*) were abundant at T1. At later time points these bacteria decreased in relative abundance, and *Firmicutes* most closely related to *Desulfotomaculum* and other *Peptococcaceae* increased (Figure 2; Figure SI-3C). The un-amended sediment community differs substantially from the acetate-amended communities and does not contain abundant (>1%) *Desulfuromonadales* or *Peptococcaceae*.[27,29]

The results demonstrate the presence of abundant bacteria that are phylogenetically similar to known Fe(III) reducers (*Geobacter* and other *Desulfuromonadales* bacteria, *Rhodoferax*, *Desulfosporosinus*)[32] in the T1 reactors. In reactors T2 and T3, the proportion of bacteria closely related to known sulfate-reducers increased substantially. Potential SRB include the *Deltaproteobacteria Desulfocapsa* and *Desulfobulbaceae* and the *Firmicutes* within the *Peptococcaceae*, *Desulfosporosinus* and *Desulfotomaculum*.[41−44] The progression from Fe(III)- to sulfate-reducing community occurred earlier in the bottoms (Infl) section of columns than in the tops (Effl), as acetate-amended groundwater was pumped up through the columns from bottom to top. Consequently, the community at the base of each column had access to higher concentrations of acetate throughout the experiment.

While there is no unique gene indicative of uranium reduction, acetate-enriched *Geobacter* species, which persisted throughout the amendment period, represent strong candidates for enzymatic Fe(III) and uranium reduction within the aquifer (e.g., ref 45). This is particularly likely during early amendment, when they were relatively more abundant. Even so, uranium reduction may also be attributed to other enriched bacteria. Some *Desulfosporosinus* and *Desulfotomaculum* species, for example, can reduce uranium.[46,47]

3.2. Characterization of U(IV) Products. Aqua regia sediment digestions revealed large differences in total uranium accumulated in sediments as a function of both reactor (T1−T3) and position within an individual reactor (top or bottom). Total uranium concentrations in the sediments vary from near zero to approximately 1 μmol of U per gram of sediment. Generally, more uranium was accumulated in the bottom sections of the reactors, where the influent groundwater containing acetate and uranium entered (Figure 3), and where conditions were more reducing than in the effluent sections of the same columns. There was also more uranium as columns became more reduced, i.e., T3 > T2 > T1. This phenomenon is likely due to a combination of longer reaction times and faster U accumulation rates under sulfate reduction possibly involving biogenic iron sulfide minerals such as mackinawite.[7,10]

Uranium XAS data were collected for the influent and effluent sections of reactors T1 and T3 and the influent section of T2. XANES data indicate that between 75 and 100% of the total uranium pool is present as U(IV) species (Figure SI-4). Despite large differences in the total sediment uranium concentration (Figure 3), time of reaction, and redox conditions (Figures 1 and 2) among the reacted sediments, the U EXAFS spectra are similar to one another (Figure 4; Supporting Information, Table SI-1, Figures SI-5 and SI-6). In particular, all spectra contain a clear and reasonably strong signature of P (or C) shells at ca. 3.1 and 3.7 Å that is consistent with noncrystalline U(IV) associated with biomass.[4,5,8] The presence of a small U−U peak at 3.8−3.9 Å implies that a small fraction of U(IV) in the samples is present as uraninite.[2,48] Uraninite is produced following the reaction of U(VI) with a variety of sulfate-reducing, metal-reducing, and other bacteria[45,49−52] and with abiotic reductants including

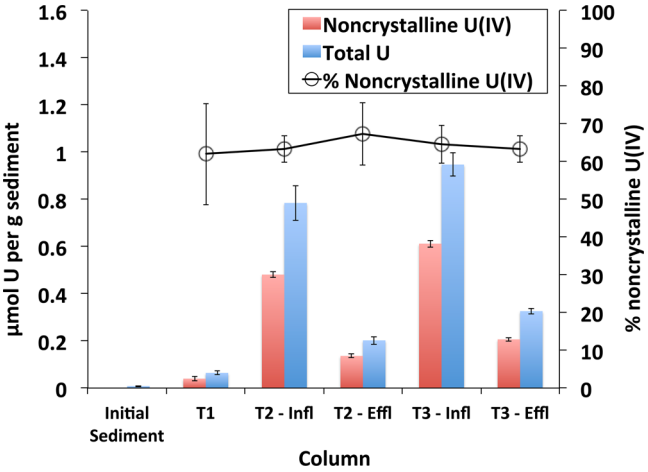

Figure 3. Uranium quantification in sediments, including bicarbonate-extracted noncrystalline U(IV) species (red bars) and total U (blue bars) from aqua regia digests, reported in μmol of U per g of sediment. The uranium quantification for reactor T1 represents an average over the entire column, whereas T2 and T3 were divided into influent and effluent sediment U extractions. The fraction of total U present as noncrystalline U(IV) species (black circles) is nearly constant for all sediments. Error bars represent the combined replicate and instrumental error.

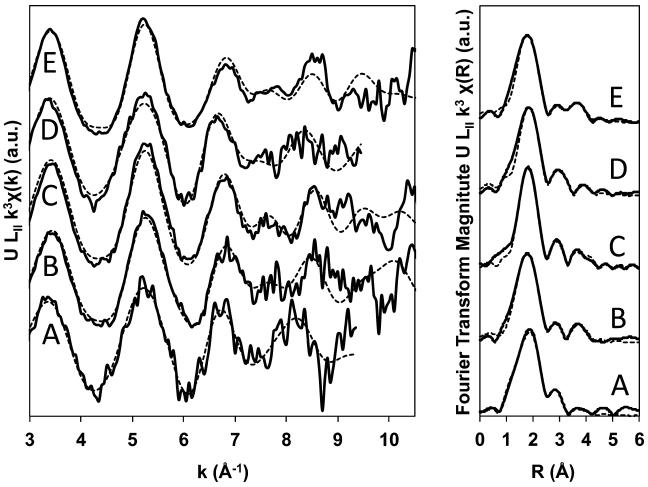

Figure 4. Uranium L_{II}-edge EXAFS and Fourier transforms for (A) column T1 Effl, (B) column T1 Infl, (C) column T2 Infl, (D) column T3 Effl, and (E) column T3 Infl.

mackinawite[10,53] and other ferrous sulfides and oxides.[48,54−56] HS^-(aq) is expected to be insignificant as a reductant for U(VI) in Rifle groundwater[24] because (bi)carbonate concentrations in the millimolar range, such as are observed in Rifle groundwater, inhibit the reduction of aqueous U(VI).[57]

The noncrystalline U(IV) fraction of the total U(IV) pool as estimated by bicarbonate extraction[15] is constant within analytical and replicate error for the top and bottom sediment sections of all three reactors and averages approximately 65%. This result is also consistent with other studies of bioreduced U(IV) species formed in laboratory[58] and field[7] experiments that use sediments from the Rifle field site. Sharp et al.[58] conducted laboratory column experiments with Rifle IFRC sediments and amended a solution containing 15 mM acetate, 55 μM uranyl acetate, and 30 mM bicarbonate until iron-reducing conditions were achieved. Sulfate reduction was not reached because sulfate was not added to the influent solution. They observed an immobilized U pool in the sediments dominated by noncrystalline U(IV), suggesting that laboratory column studies may be reasonable proxies for field studies such as ours.

The extraction and EXAFS results suggest that the U(IV) species remain dominated by noncrystalline U(IV) through metal-reducing and deep into sulfate-reducing conditions. The apparent constancy in U(IV) speciation implies a constancy in the mechanism(s) of reduction. Similar to Williams et al.,[20] we note that *Geobacter* spp. are present throughout iron- and sulfate-reducing conditions (Figure 2). Since *Geobacter* and potentially other U(VI)-reducing species are active across widely ranging redox conditions, the U(VI) removal mechanism(s) they employ may be operable and produce similar U(IV) products throughout. However, the presence of *Geobacter* cannot explain the strongly increased uranium accumulation under sulfate-reducing conditions. Another mechanism is thus inferred to be present.

While we cannot deduce a specific reaction mechanism or set of mechanisms to reconcile these results, we note that the presence of bacterial biomass is a constant throughout the experimental conditions. Bargar et al.[7] proposed a generalized reaction pathway in which the presence of bacterial biomass played a key role as a strong U(VI) binding substrate. According to this model, U(VI) bound to phosphoryl sites or phosphate groups in biomass could be reduced to U(IV) by electrons conferred via shuttles (soluble inorganic or organic shuttles or conductive pilli, or combinations thereof). U(IV) reduced in this fashion would remain complexed to biomass functional groups as noncrystalline U(IV). Stylo et al.,[13] using single species cultures, further demonstrated that solution geochemistry controlled the viability of *Shewanella* cells and their ability to produce exopolymers during U(VI) reduction in Rifle composition groundwater. Exopolymer production was directly related to a larger fraction of non-crystalline U(IV) in the overall reduced uranium pool. This model could help to explain the relative abundance of noncrystalline U(IV) observed in the present study across strongly contrasting biogeochemical regimes. In any case, so long as reducing agents, electron shuttles, and microbial exopolymers are present that can bind and reduce U(VI), then noncrystalline U(IV) is likely to be produced.

3.3. Environmental Implications. Although groundwater geochemistry has been shown to influence the speciation of U(IV) formed in sediments (e.g., refs 6, 13), this study indicates that factors including the sub-surface redox conditions, dominant microbial community and physiology, grain-coating mineralogy, inorganic reducing agents, and total U accumulated in the sediments do not dictate the appearance of noncrystalline U(IV) within the range of geochemical and microbial conditions tested here.

Driving an aquifer into sulfate-reducing conditions during bioremediation may be a sound strategy to increase the stability of U(VI) reduction to U(IV) species, i.e., via association with FeS, particularly as this does not appear to impact the speciation of the resulting U(IV) products. As long as reducing conditions are maintained and in the absence of elevated aqueous carbonate concentrations, U(IV) should remain immobile, even if present as noncrystalline U(IV) species. However, if the groundwater chemistry changes, the high fraction of noncrystalline U(IV) species, shown to be more easily mobilized and oxidized than uraninite U(IV),[12] could be

of concern. Future studies should examine the impact of time and of different aquifer geochemistry and mineralogy on U(IV) speciation, to further constrain field parameters that impact U(IV) speciation after aquifer biostimulation.

■ ASSOCIATED CONTENT

Supporting Information

Further details of the EXAFS fitting procedures, and Figures S1−S6 and Tables S1 and S2, as described in the text. This material is available free of charge via the Internet at http://pubs.acs.org.

■ AUTHOR INFORMATION

Corresponding Author

*Phone: (650)926-4949; e-mail: bargar@slac.stanford.edu.

Present Addresses

[⊗]D.S.A.: Department of Earth and Atmospheric Sciences, University of Alberta, Edmonton, AB, T6G 2E3 Canada

[#]J.M.C.: Department of Civil Engineering, University of New Mexico, Albuquerque, NM 87106, USA

[∇]K.M.H.: Department of Ecology and Evolution, University of Chicago, Chicago, IL 60637, USA

Notes

The authors declare no competing financial interest.

■ ACKNOWLEDGMENTS

We thank Drs. Christopher S. Miller and Kelly W. Wrighton and Prof. Jillian F. Banfield for their assistance with the microbial community analyses. Work carried out at EPFL was funded by Swiss NSF grants No. 20021-113784 and 200020-126821, SNSF International Co-operation grant No. IZK0Z2-12355, and SNSF International Short Visits grant No. IZK0Z2-133214. Field operations, analyses, and salary support for Alessi, Bargar, Lezama-Pacheco, Janot, and Cerrato was provided by the SLAC Science Focus Area funded by the U.S. Department of Energy Subsurface Biogeochemical Research program (FWP 10094). D.S.A. was partially supported by a Marie Curie International Incoming Fellowship from the European Commission, grant FP7-PEOPLE-2009-IIF-254143. Portions of this research were carried out at the Stanford Synchrotron Radiation Lightsource, a national user facility operated by Stanford University on behalf of the U.S. Department of Energy (DOE), Office of Basic Energy Sciences. The SSRL Structural Molecular Biology Program is supported by the DOE, Office of Biological and Environmental Research, and by the National Institutes of Health, National Center for Research Resources, Biomedical Technology Program. The Rifle Integrated Field Research Challenge (IFRC, Rifle, CO, USA) site was supported by the U.S. Department of Energy, Biological and Environmental Research, Subsurface Biogeochemical Research program. Contributions by the Lawrence Berkeley National Laboratory were supported through its Sustainable Systems Scientific Focus Area under contract DE-AC02-05CH11231. Sequencing was performed at the DNA Technologies Core Facility, Genome Center, University of California, Davis, CA, USA.

■ REFERENCES

(1) Williams, K. H.; Bargar, J. R.; Lloyd, J. R.; Lovley, D. R. Bioremediation of uranium-contaminated groundwater: a systems approach to subsurface biogeochemistry. *Curr. Opin. Biotechnol.* **2013**, *24*, 489−497.

(2) Schofield, E. J.; Veeramani, H.; Sharp, J. O.; Suvorova, E.; Bernier-Latmani, R.; Mehta, A.; Stahlman, J.; Webb, S. M.; Clark, D. L.; Conradson, S. D.; Ilton, E. S.; Bargar, J. R. Structure of biogenic uraninite produced by Shewanella oneidensis strain MR-1. *Environ. Sci. Technol.* **2008**, *42*, 7898−7904.

(3) Ulrich, K.-U.; Ilton, E. S.; Veeramani, H.; Sharp, J. O.; Bernier-Latmani, R.; Schofield, E. J.; Bargar, J. R.; Giammar, D. E. Comparative dissolution kinetics of biogenic and chemogenic uraninite under oxidizing conditions in the presence of carbonate. *Geochim. Cosmochim. Acta* **2009**, *73*, 6065−6083.

(4) Bernier-Latmani, R.; Veeramani, H.; Dalla Vecchia, E.; Junier, P.; Lezama-Pacheco, J. S.; Suvorova, E. I.; Sharp, J. O.; Wigginton, N. S.; Bargar, J. R. Non-uraninite products of microbial U(VI) reduction. *Environ. Sci. Technol.* **2010**, *44* (24), 9456−9462.

(5) Fletcher, K. E.; Boyanov, M. I.; Thomas, S. H.; Wu, Q.; Kemner, K. M.; Löffler, F. E. U(VI) reduction to mononuclear U(IV) by Desulfitobacterium species. *Environ. Sci. Technol.* **2010**, *44* (12), 4705−4709.

(6) Boyanov, M. I.; Fletcher, K. E.; Kwon, M. J.; Rui, X.; O'Loughlin, E. J.; Löffler, F. E.; Kemner, K. M. Solution and microbial controls on the formation of reduced U(VI) species. *Environ. Sci. Technol.* **2011**, *45* (19), 8336−8344.

(7) Bargar, J. R.; Williams, K. H.; Campbell, K. M.; Long, P. E.; Stubbs, J. E.; Suvorova, E. I.; Lezama-Pacheco, J. S.; Alessi, D. S.; Stylo, M.; Webb, S. M.; Davis, J. A.; Giammar, D. E.; Blue, L. Y.; Bernier-Latmani, R. Uranium redox transition pathways in acetate-amended sediments. *Proc. Natl. Acad. Sci. U.S.A.* **2013**, *110*, 4506−4511.

(8) Alessi, D. S.; Lezama-Pacheco, J. S.; Stubbs, J. E.; Janousch, M.; Bargar, J. R.; Persson, P.; Bernier-Latmani, R. The product of microbial uranium reduction includes multiple species with U(IV)-phosphate coordination. *Geochim. Cosmochim. Acta* **2014**, *131*, 115−127.

(9) Veeramani, H.; Alessi, D. S.; Suvorova, E. I.; Lezama-Pacheco, J. S.; Stubbs, J. E.; Sharp, J. O.; Dippon, U.; Kappler, A.; Bargar, J. R.; Bernier-Latmani, R. Products of abiotic U(VI) reduction by biogenic magnetite and vivianite. *Geochim. Cosmochim. Acta* **2011**, *75*, 2512−2528.

(10) Veeramani, H.; Scheinost, A. C.; Monsegue, N.; Qafoku, N. P.; Kukkapadu, R.; Newville, M.; Lanzirotti, A.; Pruden, A.; Murayama, M.; Hochella, M. F. Abiotic reductive immobilization of U(VI) by biogenic mackinawite. *Environ. Sci. Technol.* **2013**, *47*, 2361−2369.

(11) Latta, D. E.; Mishra, B.; Cook, R. E.; Kemner, K. M.; Boyanov, M. I. Stable U(IV) complexes form at high-affinity mineral surface sites. *Environ. Sci. Technol.* **2014**, *48* (3), 1683−1691.

(12) Cerrato, J. M.; Ashner, M. N.; Alessi, D. S.; Lezama-Pacheco, J. S.; Bernier-Latmani, R.; Bargar, J. R.; Giammar, D. E. Relative reactivity of biogenic and chemogenic uraninite and biogenic noncrystalline U(IV). *Environ. Sci. Technol.* **2013**, *47* (17), 9756−9763.

(13) Stylo, M.; Alessi, D. S.; Shao, P. P.; Lezama-Pacheco, J. S.; Bargar, J. R.; Bernier-Latmani, R. Biogeochemical controls on the product of microbial U(VI) reduction. *Environ. Sci. Technol.* **2013**, *47* (21), 12351−12358.

(14) Druhan, L. L.; Steefel, C. I.; Molins, S.; Williams, K. H.; Conrad, M. E.; Depaolo, D. J. Timing the onset of sulfate reduction over multiple subsurface acetate amendments by measurement and modeling of sulfur isotope fractionation. *Environ. Sci. Technol.* **2012**, *46* (16), 8895−8902.

(15) Alessi, D. S.; Uster, B.; Veeramani, H.; Suvorova, E. I.; Lezama-Pacheco, J. S.; Stubbs, J. E.; Bargar, J. R.; Bernier-Latmani, R. Quantitative separation of monomeric U(IV) from UO2 in products of U(VI) reduction. *Environ. Sci. Technol.* **2012**, *46* (11), 6150−6157.

(16) Long, P. E. Microbiological, Geochemical and Hydrologic Processes Controlling Uranium Mobility: An Integrated Field Scale Subsurface Research Challenge Site at Rifle, Colorado. February 2009 to January 2010, Annual Report, PNNL-19167; Subsurface Biogeochemistry Research Program, U.S. Department of Energy, Office of Science, Richland, WA, 2010.

(17) Moon, H. S.; McGuiness, L.; Kukkadapu, R. K.; Peacock, A. D.; Komlos, J.; Kerkhof, L. J.; Long, P. E.; Jaffé, P. R. Microbial reduction of uranium under iron- and sulfate-reducing conditions: Effect of

amended goethite on microbial community composition and dynamics. *Wat. Res.* **2010**, *44*, 4015−4028.
(18) Campbell, K. M.; Davis, J. A.; Bargar, J.; Giammar, D.; Bernier-Latmani, R.; Kukkadapu, R.; Williams, K. H.; Veeramani, H.; Ulrich, K-. U.; Stubbs, J.; Yabusaki, S.; Figueroa, L.; Lesher, E.; Wilkins, M. J.; Wilkins, M.; Peacock, A.; Long, P. E. Composition, stability and measurement of reduced uranium phases for groundwater bioremediation at Old Rifle, CO. *Appl. Geochem.* **2011**, *26*, S163−S169.
(19) Yabusaki, S. B.; Fang, Y.; Long, P. E.; Resch, C. T.; Peacock, A. D.; Komlos, J.; Jaffe, P. R.; Morrison, S. J.; Dayvault, R.; White, D. C.; Anderson, R. T. Uranium removal from groundwater via in situ biostimulation: Field-scale modeling of transport and biological processes. *J. Contam. Hydrol.* **2007**, *93*, 216−235.
(20) Williams, K. H.; Long, P. E.; Davis, J. A.; Wilkins, M. J.; N'Guessan, A. L.; Steefel, C. I.; Yang, L.; Newcomer, D.; Spane, F. A.; Kerkhof, L. J.; McGuinness, L.; Dayvault, R.; Lovley, D. R. Acetate availability and its influence on sustainable bioremediation of uranium-contaminated groundwater. *Geomicrobiol. J.* **2011**, *28* (5−6), 519−539.
(21) Bao, C.; Wu, H.; Li, L.; Newcomer, D.; Long, P. E.; Williams, K. H. Uranium bioreduction rates across scales: Biogeochemical hot moments and hot spots during a biostimulation experiment at Rifle, Colorado. *Environ. Sci. Technol.* **2014**, *48*, 10116−10127.
(22) Department of Energy (2012) Legacy Management Geospatial Environmental Mapping System. Available at http://gems.lm.doe.gov/imf/sites/gems_continental_us/jsp/launch.jsp. Accessed May 1, 2014.
(23) Anderson, R. T.; Vrionis, H. A.; Ortiz-Bernad, I.; Resch, C. T.; Long, P. E.; Dayvault, R.; Karp, K.; Marutzky, S.; Metzler, D. R.; Peacock, A.; White, D. C.; Lowe, M.; Lovley, D. R. Stimulating the in situ activity of Geobacter species to remove uranium from the groundwater of a uranium-contaminated aquifer. *Appl. Environ. Microbiol.* **2003**, *69*, 5884−5891.
(24) Long, P. E. Microbiological, Geochemical and Hydrologic Processes Controlling Uranium Mobility: An Integrated Field Scale Subsurface Research Challenge Site at Rifle, Colorado. February 2010 to January 2011, Annual Report, PNNL-20200; Subsurface Biogeochemistry Research Program, Department of Energy Office of Science, Richland, WA, 2011.
(25) Stoliker, D. L.; Campbell, K. M.; Fox, P. M.; Singer, D. M.; Kaviani, N.; Carey, M.; Peck, N. E.; Bargar, J. R.; Kent, D. B.; Davis, J. A. Evaluating chemical extraction techniques for the determination of uranium oxidation state in reduced aquifer sediments. *Environ. Sci. Technol.* **2013**, *47* (16), 9225−9232.
(26) Kelly, S. D.; Hesterberg, D.; Ravel, B..Analysis of Soils and Minerals Using X-ray Absorption Spectroscopy. In *Methods of Soil Analysis. Part 5. Mineralogical Methods*; Ulery, A. L., Drees, R., Eds.; Soil Science Socitey of America: Madison, WI, 2008; pp 387− 463.
(27) Handley, K. M.; Wrighton, K. C.; Miller, C. S.; Wilkins, M. J.; Kantor, R. S.; Williams, K. H.; Gilbert, J. A.; Long, P. E.; Banfield, J. F. Disturbed subsurface microbial communities follow equivalent trajectories despite different structural starting points. *Environ. Microbiol.* **2014**, DOI: 10.1111/1462-2920.12467.
(28) Goltsman, D. S. A.; Denef, V. J.; Singer, S. W.; VerBerkmoes, N. C.; Lefsrud, M.; Mueller, R. S.; Dick, G. J.; Sun, C. L.; Wheeler, K. E.; Zemla, A.; Baker, B. J.; Hauser, L.; Land, M.; Shah, M. B.; Thelen, M. P.; Hettich, R. L.; Banfield, J. F. Community genomic and proteomic analyses of chemoautotrophic iron-oxidizing "Leptospirillium rubarum" (Group II) and "Leptospirillum ferrodiazotrophum" (Group III) bacteria in acid mine drainage biofilms. *Appl. Environ. Microbiol.* **2009**, *75* (13), 4599−4615.
(29) Miller, C. S.; Handley, K. M.; Wrighton, K. C.; Frischkorn, K. R.; Thomas, B. C.; Banfield, J. F. Deep sequencing and assembly of full-length 16S rRNA amplicons uncovers broad bacterial diversity in subsurface sediments. *PLoS One* **2013**, *8*, No. e56018.
(30) Wang, Q.; Garrity, G. M.; Tiedje, J. M. Naive Bayesian classifier for rapid assignment of rRNA sequences into the new bacterial taxonomy. *Appl. Environ. Microbiol.* **2007**, *73* (16), 5261−5267.
(31) Altschul, S. F.; Gish, W.; Miller, W.; Myers, E. W.; Lipman, D. J. Basic local alignment search tool. *J. Mol. Biol.* **1990**, *215*, 403−410.
(32) Price, M. N.; Dehal, P. S.; Arkin, A. P. FastTree: Computing large minimum evolution trees with profiles instead of a distance matrix. *Mol. Biol. Evol.* **2009**, *26* (7), 1641−1650.
(33) Hamady, M.; Lozupone, C.; Knight, R. Fast UniFrac: facilitating high-throughput phylogenetic analyses of microbial communities including analysis of pyrosequencing and PhyloChip data. *ISME J.* **2010**, *4* (1), 17−27.
(34) Webb, S. M. SIXPACK: a graphical user interface for XAS analysis using IFEFFIT. *Phys. Scr.* **2005**, *T115*, 1011−1014.
(35) Ravel, B.; Newville, M. Athena, Artemis, Hephaestus: Data Analysis for X-Ray Absorption Spectroscopy Using Ifeffit. *J. Synchrotron Radiat.* **2005**, *12*, 537−541.
(36) Rehr, J. J.; Albers, R. C.; Zabinsky, S. I. High-order multiple-scattering calculations of X-ray-absorption fine-structure. *Phys. Rev. Lett.* **1992**, *69*, 3397−3400.
(37) Li, L.; Steefel, C. I.; Williams, K. H.; Wilkins, M. J.; Hubbard, S. S. Mineral transformation and biomass accumulation associated with uranium bioremediation at Rifle, Colorado. *Environ. Sci. Technol.* **2009**, *43* (14), 5429−5435.
(38) Fang, Y.; Yabusaki, S. B.; Morrison, S. J.; Amonette, J. P.; Long, P. E. Multicomponent reactive transport modeling of uranium bioremediation field experiments. *Geochim. Cosmochim. Acta* **2009**, *73* (20), 6029−6051.
(39) Fox, P. M., Davis, J. A., Hay, M. B., Conrad, M. E., Campbell, K. M., Williams, K. H., Long, P. E. (**2012**) Rate-limited U(VI) desorption during a small-scale tracer test in a heterogeneous uranium-contaminated aquifer. *Wat. Resour. Res. 48*, article W05512.
(40) Lovley, D. R.; Holmes, D. E.; Nevin, K. P. In *Dissimilatory Fe(III) and Mn(IV) reduction*; Advances in Microbial Physiology *49*; Poole, R. K., Ed.; Academic Press Ltd/Elsevier Science Ltd: London, 2004; pp 219−286.
(41) Janssen, P. H.; Schuhmann, A.; Bak, F.; Liesack, W. Disproportionation of inorganic sulfur compounds by the sulfate-reducing bacterium Desulfocapsa thiozymogenes gen nov, sp nov. *Arch. Microbiol.* **1996**, *166* (3), 184−192.
(42) Lien, T.; Madsen, M.; Steen, I. H.; Gjerdevik, K. Desulfobulbus rhabdoformis sp. nov., a sulfate reducer from a water-oil separation system. *Int. J. Syst. Bacteriol.* **1998**, *48*, 469−474.
(43) Ramamoorthy, S.; Sass, H.; Langner, H.; Schumann, P.; Kroppenstedt, R. M.; Spring, S.; Overmann, J.; Rosenzweig, R. F. Desulfosporosinus lacus sp nov., a sulfate-reducing bacterium isolated from pristine freshwater lake sediments. *Int. J. Syst. Evolutionary Microbiol.* **2006**, *56*, 2729−2736.
(44) Haouari, O.; Fardeau, M. L.; Cayol, J. L.; Casiot, C.; Elbaz-Poulichet, F.; Hamdi, M.; Joseph, M.; Ollivier, B. Desulfotomaculum hydrothermale sp nov., a thermophilic sulfate-reducing bacterium isolated from a terrestrial Tunisian hot spring. *Int. J. Syst. Evolutionary Microbiol.* **2008**, *58*, 2529−2535.
(45) Anderson, R. T.; Vrionis, H. A.; Ortiz-Bernad, I.; Resch, C. T.; Long, P. E.; Dayvault, R.; Karp, K.; Marutzky, S.; Metzler, D. R.; Peacock, A.; White, D. C.; Lowe, M.; Lovley, D. R. Stimulating the *in situ* activity of *Geobacter* species to remove uranium from the groundwater of a uranium-contaminated aquifer. *Appl. Environ. Microbiol.* **2003**, *69*, 5884−5891.
(46) Suzuki, Y.; Kelly, S. D.; Kemner, K. M.; Banfield, J. F. Enzymatic U(VI) reduction by Desulfosporosinus species. *Radiochim. Acta* **2004**, *92*, 11−16.
(47) Wall, J. D.; Krumholz, L. R. Uranium reduction. *Annu. Rev. Microbiol.* **2006**, *60*, 149−166.
(48) O'Loughlin, E. J.; Kelly, S. D.; Cook, R. E.; Csencsits, R.; Kemner, K. M. Reduction of uranium(VI) by mixed iron(II)/iron(III) hydroxide (Green Rust): Formation of UO2 nanoparticles. *Environ. Sci. Technol.* **2003**, *37*, 721−727.
(49) Lovley, D. R.; Phillips, E. J. P.; Gorby, Y. A.; Landa, E. R. Microbial reduction of uranium. *Nature* **1991**, *350*, 413−416.
(50) Kelly, S. D.; Wu, W-. M.; Yang, F.; Criddle, C. S.; Marsh, T. L.; O'Loughlin, E. J.; Ravel, B.; Watson, D.; Jardine, P. M.; Kemner, K. M. Uranium transformations in static microcosms. *Environ. Sci. Technol.* **2009**, *44* (1), 236−242.

(51) Ray, A. E.; Bargar, J. R.; Sivaswamy, V.; Dohnalkova, A.; Fujita, Y.; Peyton, B. M.; Magnuson, T. S. Evidence for multiple modes of uranium immobilization by an anaerobic bacterium. *Geochim. Cosmochim. Acta* **2011**, *75*, 2684−2695.
(52) Sivaswamy, V.; Boyanov, M. I.; Peyton, B. M.; Viamajala, S.; Gerlach, R.; Apel, W. A.; Sani, R. K.; Dohnalkova, A.; Kemner, K. M.; Borch, T. Multiple mechanisms of uranium immobilization by Cellulomonas sp. strain ES6. *Biotechnol. Bioeng.* **2011**, *108*, 264−276.
(53) Hyun, S. P.; Davis, J. A.; Sun, K.; Hayes, K. F. Uranium (VI) reduction by Fe(II) monosulfide, mackinawite. *Environ. Sci. Technol.* **2012**, *46*, 3369−3376.
(54) Wersin, P.; Hochella, M. F.; Persson, P.; Redden, G.; Leckie, J. O.; Harris, D. W. Interaction between aqueous uranium (VI) and sulfide minerals: Spectroscopic evidence for sorption and reduction. *Geochim. Cosmochim. Acta* **1994**, *58* (13), 2829−2843.
(55) Descostes, M.; Schlegel, M. L.; Eglizaud, N.; Descamps, F.; Miserque, F.; Simoni, E. Uptake of uranium and trace elements in pyrite (FeS_2). *Geochim. Cosmochim. Acta* **2010**, *74* (5), 1551−1562.
(56) Latta, D. E.; Boyanov, M. I.; Kemner, K. M.; O'Loughlin, E. J.; Scherer, M. M. Abiotic reduction of uranium by Fe(II) in soil. *Appl. Geochem.* **2012**, *27*, 1512−1524.
(57) Hua, B.; Xu, H.; Terry, J.; Deng, B. Kinetics of uranium(VI) reduction by hydrogen sulfide in anoxic aqueous systems. *Environ. Sci. Technol.* **2006**, *40* (15), 4666−4671.
(58) Sharp, J. O.; Lezama-Pacheco, J. S.; Schofield, E. J.; Junier, P.; Ulrich, K.-U.; Chinni, S.; Veeramani, H.; Margot-Roquier, C.; Webb, S. M.; Tebo, B. M.; Giammar, D. E.; Bargar, J. R.; Bernier-Latmani, R. Uranium speciation and stability after reductive immobilization in aquifer sediments. *Geochim. Cosmochim. Acta* **2011**, *75*, 6497−6510.